Mem. S.A.It. Vol. 77, 750

Memorie della

Black holes and nuclear dynamics

D. Merritt

Department of Physics, Rochester Institute of Technology, Rochester, NY 14623, USA
e-mail: merritt@astro.rit.edu

Abstract. Supermassive black holes inhabit galactic nuclei, and their presence influences in crucial ways the evolution of the stellar distribution. The low-density cores observed in bright galaxies are probably a result of black hole infall, while steep density cusps like those at the Galactic center are a result of energy exchange between stars moving in the gravitational field of the single black hole. Loss-cone dynamics are substantially more complex in galactic nuclei than in collisionally-relaxed systems like globular clusters due to the wider variety of possible geometries and orbital populations. The rate of star-black hole interactions has begun to be constrained through observations of energetic events associated with stellar tidal disruptions.

1. Introduction

The association of supermassive black holes (SBHs) with galactic nuclei began even before their observational confirmation, when Zel'dovich & Novikov (1964) and Salpeter (1964) first discussed the growth of massive objects at the centers of galaxies. Since then, the mutual interaction of SBHs and stars has played a central role both in the detection and mass determination of SBHs (Ferrarese & Ford 2005), and also in our theoretical understanding of how nuclei form and evolve. The realization that galactic spheroids grow through mergers added an interesting complication to this picture, since galaxy mergers imply the formation of binary SBHs (Begelman, Blandford & Rees 1980), which can influence the stellar distribution on larger spatial scales than single SBHs, and which may be directly or indirectly connected with nuclear activity (Komossa 2003).

Send offprint requests to: D. Merritt

2. Binary Black Holes and Cores

Galaxy mergers bring SBHs together, and unless the binary SBHs themselves coalesce, ejections will occur when a third SBH is deposited into a nucleus containing an uncoalesced binary (Mikkola & Valtonen 1990; Volonteri, Haardt & Madau 2003). Such events can not be too frequent or the tight, empirical correlations between SBH masses and galaxy properties (Ferrarese & Merritt 2000; Graham et al. 2001; Marconi & Hunt 2003) would be violated (Haehnelt & Kauffmann 2002).

Ultimately, coalescence is driven by emission of gravitational waves, but this process only becomes efficient when separations fall below $\sim 10^{-3}$ pc. By comparison, the natural separation between two SBHs of mass m_1 and m_2 in a galactic nucleus is

$$a_h \equiv \frac{G\mu}{4\sigma^2} \approx 2.7\,\mathrm{pc}\frac{q}{(1+q)^2}M_{\bullet,8}\sigma_{200}^{-2} \qquad (1)$$

where $M_\bullet = m_1 + m_2$, $\mu = m_1 m_2/M_\bullet$ is the reduced mass, $q = m_2/m_1 \leq 1$ is the mass ra-

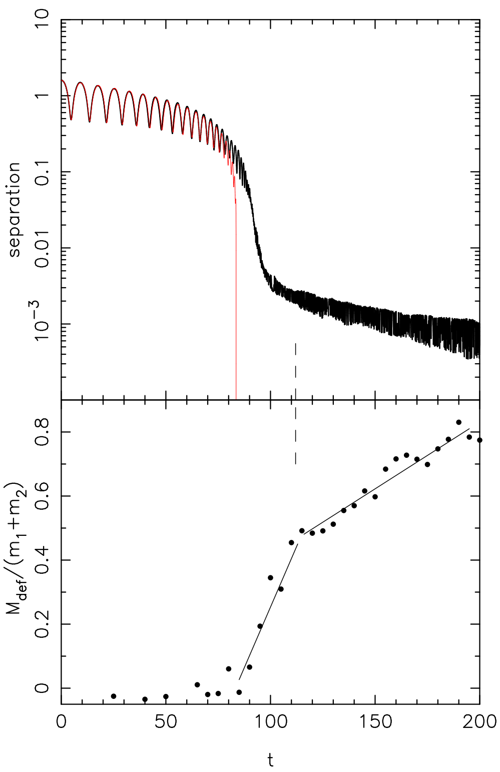

Fig. 1. Short-term evolution of binary black holes in spherical galaxies. *Upper panel:* Thick (black) line shows infall of a hole of mass m_2 into a nucleus containing a hole of mass $m_1 = 10m_2$. Thin (red) line is the orbital decay predicted by the dynamical friction equation, assuming an unchanging galaxy. The vertical dashed line indicates the time when $a \approx a_h$. *Lower panel:* Evolution of the mass deficit, i.e. the mass displaced by the binary, in units of the combined mass of the two black holes. The evolution slows at $a \approx a_h$ due to ejection of stars on orbits that intersect the binary, and thereafter the evolution rate is strongly dependent on the number N of particles used to represent the galaxy (here, $N = 2 \times 10^5$). For much larger N, the binary would stall at $a \approx a_h$ (see Fig. 2).

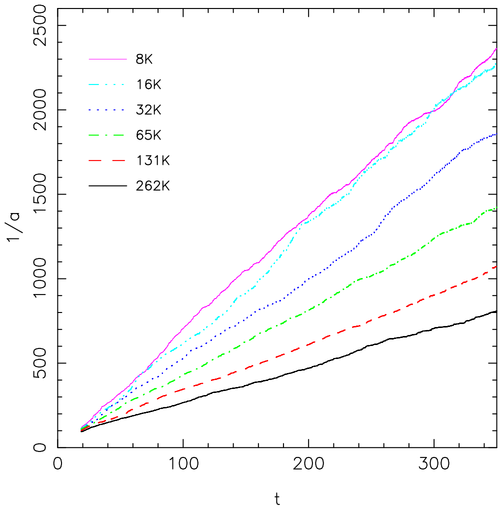

Fig. 2. Long-term evolution of binary black holes in spherical galaxies. Each curve shows the evolution of the inverse semi-major axis of an equal-mass binary in a spherical galaxy with an initially power-law nuclear density profile. Curves were obtained by averaging multiple N-body integrations with the same N. As N increases, the binary's hardening rate drops, implying very slow evolution past $a \approx a_h$ in a real galaxy (adapted from Merritt, Mikkola & Szell 2006).

tio, $M_{\bullet,8} = M_\bullet/10^8 M_\odot$, and σ_{200} is the nuclear velocity dispersion in units of 200 km s^{-1}. A binary with semi-major axis $a \approx a_h$ is "hard," i.e. its binding energy per unit mass is $\sim \sigma^2$ and its total binding energy E_h is a fraction $\sim M_\bullet/M_{gal} \approx 10^{-3}$ that of the host galaxy.

The separation a_h is natural one since a binary with $a \lesssim a_h$ efficiently ejects stars on intersecting orbits (Mikkola & Valtonen 1992; Quinlan 1996). In a spherical or axisymmetric galaxy, the total mass associated with stars on such orbits is small, $\lesssim M_\bullet$, and once the binary has ejected these stars, its evolution greatly slows. This is the "final parsec problem." In N-body simulations (e.g. Milosavljevic & Merritt 2001, Makino & Funato 2004), the binary often *does* evolve past $a \approx a_h$ but at a rate that is strongly N-dependent (Figs. 1,2). This reflects the fact that processes like gravitational scattering and Brownian motion that can refill a binary's loss cone are $m_\star$-dependent.

Since the efficiency of loss-cone repopulation in real galaxies is uncertain and may be low, it is interesting to ask what the observable consequences would be of binaries stalling at

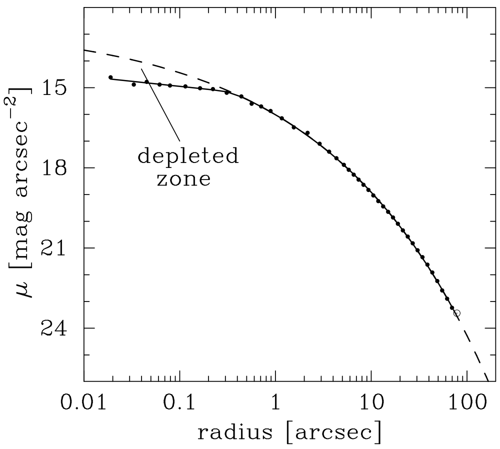

Fig. 3. Observational determination of mass deficits. Plot shows the observed surface brightness profile of NGC 3348. The dashed line is a Sersic model fit to the large-radius data. Solid line is the fit of an alternative model, the "core-Sersic" model, which fits both the inner and outer data well. The mass deficit is illustrated by the area designated "depleted zone" and the corresponding mass is roughly $3 \times 10^8 M_\odot$ (from Graham 2004).

$a \approx a_h$. Using the $M_\bullet - \sigma$ relation, Eq. (1) can be written

$$a_{h,\mathrm{pc}} \approx 0.3\, q_{0.1}\, \sigma_{200}^{2.9} \tag{2}$$

with $q_{0.1} \equiv q/0.1$. "Dual" SBHs are observed in a handful of interacting galaxies and binary quasars (Mortlock et al. 1999; Komossa et al. 2003; Ballo et al. 2004), but always with much larger separations, $\gtrsim 1$ kpc. True binaries with $a \approx a_h$ would be difficult to resolve outside the Local Group even if both SBHs were luminous. A number of active galaxies show evidence for variability with periods similar to binary orbital periods, but the variability may be a scaled-up version of the quasi-periodic oscillations associated with stellar-mass black holes and not the signature of a binary SBH (Uttley 2005).

An indirect way to track the evolution of a binary SBH is via its effects on the structure of the nucleus. The infalling hole begins displacing stars when it first becomes bound to the second, at a separation $\sim r_h \equiv GM_\bullet/\sigma^2 \approx 10M_{\bullet,8}\sigma_{200}^{-2}$ pc $\approx 15M_{\bullet,8}^{0.59}$ pc. Evolution from r_h to a_h is rapid unless the mass ratio is extreme, and the "damage" done by the binary to the nucleus can be robustly estimated from N-body simulations, independent of uncertainties about the efficiency of loss-cone refilling (Fig. 1). A standard definition of the damage is the "mass deficit" M_{def}, the difference in integrated mass between the observed density profile and the primordial (pre-merger) profile (Milosavljević et al. 2002). N-body simulations like those in Fig. 1 show that $M_{def}(a = a_h) \approx 0.5(m_1 + m_2)$, decreasing only weakly with m_2, and nearly independent of the form of the initial density profile. This is a consequence of the scaling of E_h with $m_1 + m_2$ discussed above. An interesting corollary is that the mass deficit after $\mathcal{N}$ mergers should be $\sim 0.5M_\bullet\mathcal{N}$, with $M_\bullet$ the final (i.e. current) mass of the SBH, almost independent of the details of the merger tree.

Bright ($M_B \lesssim -20.5$) elliptical galaxies always exhibit cores, regions near the center where the luminosity profile is nearly flat (Ferrarese et al. 2006 and references therein). Estimating M_{def} in a real galaxy is not straightforward however, since one does not know what the pre-existing stellar distribution was. A conservative approach is to fit a smooth function, e.g. Sérsic's law, to the outer luminosity profile and extend it inward; the mass deficit is then defined in terms of the differential profile (Fig. 3). Mass deficits derived in this way are found to be roughly equal to $M_\bullet$ (Graham 2004; Ferrarese et al. 2006) This is consistent with the relation given above if $\mathcal{N} \approx 2$, in reasonable accord with hierarchical galaxy formation models. Alternatively, if the binary evolves all the way to coalescence and if gravitational waves are emitted anisotropically during the final plunge (the "rocket" effect; Favata et al. 2004), the displaced hole will transfer energy to the nucleus before falling back to the center, increasing the mass deficit by some appreciable fraction of $M_\bullet$ (Merritt et al. 2004; Boylan-Kolchin et al. 2004).

Evolution past $a \approx a_h$ may or may not leave an additional mark on a nucleus. In small dense galaxies like M32, two-body (star-star) relaxation can repopulate a binary's loss cone at interesting rates, possibly driving the bi-

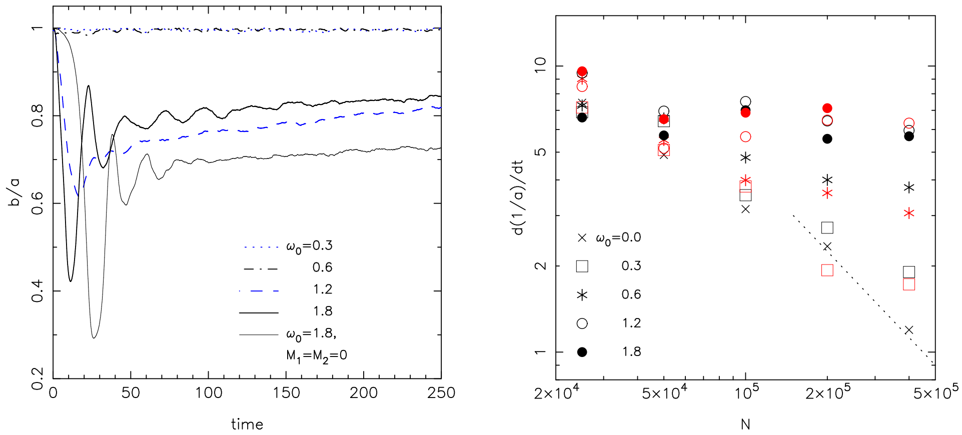

Fig. 4. Efficient merger of binary SBHs in barred galaxies. The left panel shows the evolution of the bar amplitude in a set of initially axisymmetric galaxy models with different degress of rotational support (measured by the parameter ω_0). For $\omega_0 \geq 0.6$ the models are bar-unstable. The right panel shows the hardening rate of a massive binary at the center of the galaxy. In the barred (triaxial) models, the binary's hardening rate is independent of particle number N, while in the axisymmetric models it falls roughly as N^{-1} indicating a collisionally-resupplied loss cone (adapted from Berczik et al. 2006)

nary to coalescence in $\lesssim$ 10 Gyr (Yu 2002; Milosavljevic & Merritt 2003). N-body simulations like those in Fig. 2 show that the mass deficit increases as $M_{def} \propto \ln(a_h/a)$ in such cases, so that the observed value of M_{def} does not contain much information about the final value of a. The bright elliptical galaxies that are observed to contain cores have relaxation times that are much too long for collisional loss cone repopulation to occur however. A more efficient way to drive a binary to coalescence is to imbed it in a strongly non-axisymmetric (barred or triaxial) galaxy (Merritt & Poon 2004; Holley-Bockelmann & Sigurdsson 2006). Triaxial potentials can support large populations of "centrophilic" orbits, allowing a binary to harden well past a_h by interacting with stars even in the absence of collisional loss-cone refilling (Fig. 4). Most of the stars supplying mass to the binary under these circumstances have orbital apocenters $\gg r_h$ and their depletion has almost no effect on the nuclear density profile.

A binary with $a \ll a_h$ ejects stars with velocities large enough to expel them from the galaxy. A handful of hypervelocity stars (HVSs) have been found in the Galactic halo that are candidates for ejection (Brown et al. 2005; Hirsch et al. 2005; Brown et al. 2006). These stars must have left the nucleus $\lesssim 10^8$ yr ago however, implying that a binary SBH was present until quite recently. Other models can produce HVSs in the absence of a second SBH (e.g. Hills 1988; Gualandris et al. 2005). Ejection by binary SBHs might also be responsible for populations like the intergalactic planetary nebulae observed in the Virgo cluster (Holley-Bockelmann et al. 2005). However, such models require that the binary SBHs ejecting the nebulae harden well beyond $a = a_h$, and also that the hardening is driven by star-binary interactions; both assumptions are open to question, particularly in the case of the brightest Virgo galaxies.

The nuclei of merging galaxies are expected to contain some of the largest concentrations of dense gas in the universe. Binary-gas simulations fall into two categories depending on whether the gas is modelled as "hot," i.e. having a specific kinetic energy comparable with that of the stars, or "cold," e.g. in a thin disk. The first case is much easier to treat; if the mass in gas within $\sim a_h$ is comparable to $M_\bullet$, the additional component of dynamical friction drag can bring the two SBHs together in much less than 10^9 yr (Escala et al. 2004, 2005). However it is not clear that such massive, dense accumulations of hot gas can be sustained. In the case of binary-disk interactions the difficulties are computational, e.g. resolving the gas on scales smaller than the radial wavelength of the density waves induced by the binary. Much progress in this area is to be expected in coming years.

3. Nuclear Equilibria

Once the massive binary has coalesced (or otherwise stopped interacting with stars), the stellar distribution in the nucleus can evolve to a steady state. An important distinction can be made between *collisional* nuclei, which have two-body (star-star) relaxation times less than 10 Gyr, and *collisionless* nuclei, with $T_r \gtrsim 10$ Gyr. Fig. 5 shows that $T_r(r_h)$ drops below 10 Gyr in spheroids roughly as faint as the bulge of the Milky Way.

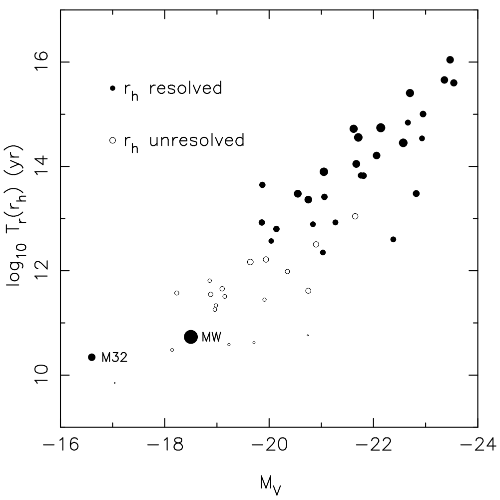

Fig. 5. Nuclear relaxation times in a sample of early-type galaxies and bulges. The size of the symbols reflects the degree to which the SBH's influence radius was resolved; filled symbols have $\theta_{r_h} > \theta_{obs}$ (resolved) and open circles have $\theta_{r_h} < \theta_{obs}$ (unresolved) (from Merritt & Szell 2005).

The morphology of collisionless nuclei is constrained only by Jean's theorem, i.e. by the requirement that the density be representable as a superposition of orbits integrated in the self-consistent potential. Collisionless equilibria can take many forms, including triaxial nuclei with chaotic orbits (Poon & Merritt 2004), as well as the simpler, axisymmetric models that are the basis for most SBH mass estimation (Gebhardt et al. 2003). A recent review is given by Merritt (2006).

In a collisional nucleus, on the other hand, exchange of energy between stars drives the phase-space density toward a characteristic form. Here we discuss the more limited class of solutions associated with collisionally-relaxed nuclei.

Gravitational encounters drive the velocity distribution of stars around a black hole toward a Maxwellian on a time scale of $\sim T_r$, but a Maxwellian velocity distribution implies an exponentially divergent mass near the hole. The existence of a region close to the black hole in which stars are captured or destroyed prevents the nucleus from reaching precise thermal equilibrium. The density must drop to zero on orbits that intersect the hole's event horizon or that pass within the tidal disruption sphere at $r = r_t$; the latter radius is most relevant here since galaxies with collisional nuclei probably always have $M_\bullet < 10^8 M_\odot$ (Fig. 5) and hence $r_t > 2GM_\bullet/c^2$.

For a single-mass population of stars moving in the Keplerian potential of a black hole, the steady-state solution to the isotropic, orbit-averaged Fokker-Planck equation in the presence of a central "sink" is approximately

$$f(E) = f_0|E|^{1/4}, \ \ \rho(r) = \rho_0 r^{-7/4}, \tag{3}$$

$$|E_h| \ll |E| \ll |E_t|, \ \ r_t \ll r \ll r_h \tag{4}$$

(Bahcall & Wolf 1976; Lightman & Shapiro 1977). Here $E_t \equiv -GM_\bullet/r_t$ and $E_h \equiv -GM_\bullet/r_h$. This is a "zero-flux" solution, i.e. it implies $F_E = 0$ at $|E_h| \ll |E| \ll |E_t|$ where F_E is the encounter-driven flux of stars in energy space. The actual flux is small but non-zero, of order

$$F_E \approx \frac{n(r_t)r_t^3}{T_r(r_t)} \propto r_t. \tag{5}$$

In other words, the flux is limited by the rate at which stars can diffuse into the disruption sphere at r_t. This flux is "small" in the sense that the one-way flux of stars in or out through a surface at $r_t \ll r \ll r_h$ is much greater; except near r_t, the inward and outward fluxes almost cancel.

The Bahcall-Wolf solution has been verified in a number of studies based on Fokker-Planck (Cohn & Kulsrud 1978), fluid (Amaro-Seoane et al. 2004), or Monte-Carlo (Marchant & Shapiro 1980; Duncan & Shapiro 1983; Freitag & Benz 2002) approximations. Most recently, advances in computer hardware (Makino et al. 2003) have made it possible to test the Bahcall-Wolf solution via direct N-body integrations, avoiding the approximations of the Fokker-Planck formalism (Preto et al. 2004; Baumgardt et al. 2004; Merritt & Szell 2005). Another advantage of this approach is that it can easily deal with complex initial conditions and nonspherical geometries, such as those set up by a binary SBH.

Fig. 6 shows a simulation of cusp destruction (by a binary SBH) followed by cusp regeneration (via the Bahcall-Wolf mechanism). The Bahcall-Wolf cusp rises above the core inside a radius $\sim 0.2r_h$ and reaches its steady-state form in a time $2-3T_r(0.2r_h)$. In the Milky Way nucleus, $0.2r_h \approx 0.7$ pc and $T_r(0.2r_h) \approx 6$ Gyr (assuming $m_\star = 0.7M_\odot$). In fact, as Fig. 6 shows, the stellar distribution at the Galactic center is close to the Bahcall-Wolf form.

Figs. 5 and 6 suggest that Bahcall-Wolf cusps should be present in many galaxies with luminosities similar to that of the Milky Way bulge, or fainter, assuming that they contain SBHs. M32 fits these criteria; the mass of its SBH is uncertain by a factor ~ 5 (Valluri et al. 2004) but even if the largest possible value is assumed, $0.2r_h \approx 0.8$ pc $\approx 0.3''$ would only barely be resolved. NGC 205 clearly contains a constant-density core but also shows no dynamical evidence of a massive black hole (Valluri et al. 2005). All other galaxies in which r_h is resolved have nuclear relaxation times $\gg 10$ Gyr (Fig. 5).

4. Loss-Cone Dynamics

As discussed above, the existence of a region $r \leq r_t$ close to the SBH where stars are destroyed has a profound influence on the steady-state distribution of stars even at $r \gg r_t$. Loss of stars is also important because of its observational consequences: tidally disrupted stars are expected to produce X- and UV radiation with luminosities of $\sim 10^{44}$ erg s^{-1} (Meszaros & Silk 1977; Rees 1990).

Once a central SBH has removed stars on orbits that intersect the disruption sphere $r = r_t$, continued supply of stars to the SBH requires some mechanism for loss-cone repopulation. The most widely discussed mechanism is gravitational encounters, which drive a diffusion in energy and angular momentum. The latter dominates the loss rate, since even a small percentage change in angular momentum can put a typical star into the loss cone (Frank & Rees 1976; Lightman & Shapiro 1977).

A large fraction of the stars within the SBH's influence radius will be deflected into r_t in one relaxation time, i.e. the loss rate is roughly $(M_\bullet/m_\star)/T_r(r_h)$. In a collisional nucleus with $M_\bullet \approx 10^6 M_\odot$, this is $\sim 10^6/(10^{10}$ yr) $\approx 10^{-4}$ yr^{-1}. A slightly more careful calculation for the tidal disruption rate in a $\rho \propto r^{-2}$ nucleus gives

$$\dot{N} \approx 7\times 10^{-4}\mathrm{yr}^{-1}\left(\frac{\sigma}{70\mathrm{km\ s}^{-1}}\right)^{7/2}\left(\frac{M_\bullet}{10^6 M_\odot}\right)^{-1} \times \left(\frac{m_\star}{M_\odot}\right)^{-1/3}\left(\frac{R_\star}{R_\odot}\right)^{1/4} \tag{6}$$

where $m_\star$ and $R_\star$ are the mass and radius of the tidally disrupted stars (Wang & Merritt 2004). Assuming $\rho \sim r^{-2}$ is reasonable since this is approximately the slope observed with the *Hubble Space Telescope* at $r \gtrsim r_h$ in the low-luminosity galaxies that dominate the event rate (Gebhardt et al. 1996).

A handful of X-ray flares have been detected that are candidates for tidal disruptions (Komossa & Greiner 1999; Komossa et al. 2004; Halpern et al. 2004). The mean disruption rate computed from this small set of events is very uncertain but is probably consistent with Eq. (6) (Donley et al. 2002). The nuclei in which tidal disruptions have occurred appear to remain luminous for 1 – 10 yr after disruption and possibly longer; in three of the observed events, the luminosity decay approx-

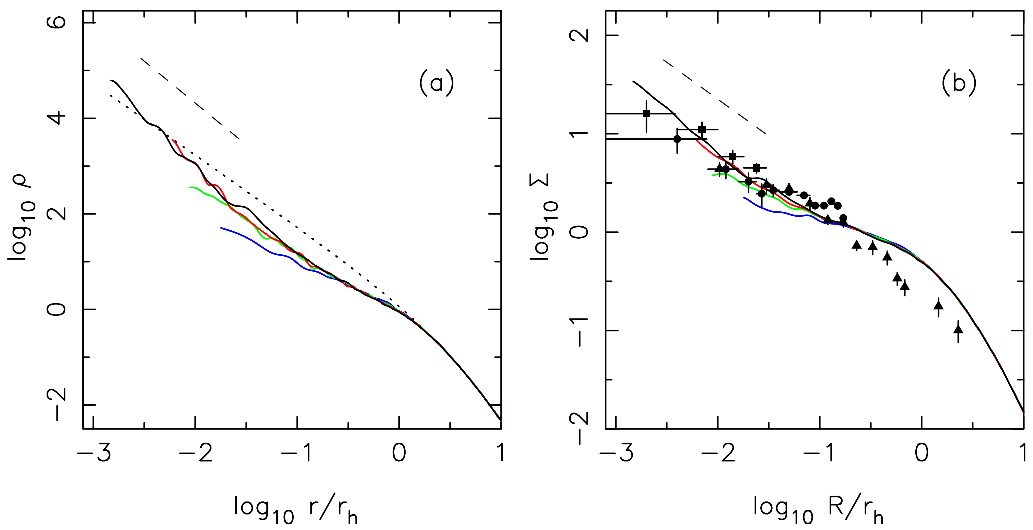

Fig. 6. Cusp regeneration. Curves show the evolution of the spatial (a) and projected (b) density profiles of an N-body model in which an initial, $\rho \sim r^{-1.5}$ density cusp (dotted line) was destroyed by infall of a second black hole of mass $m_2 = 0.5m_1$. Blue (lower) line shows the density after infall, and green, red and black lines show the evolving density after the two black holes have been merged into one; the final time is $\sim$ 10 Gyr if scaled to the Milky Way. Symbols in (b) show the observed surface density of stars near the Galactic Center (Genzel et al. 2003). Dashed lines have logarithmic slopes of -1.75 (a) and -0.75 (b), the Bahcall-Wolf "zero flux" solution (from Merritt & Szell 2005).

imately obeys the $L_x \propto t^{-5/3}$ dependence predicted if emission is produced during the fallback of stellar debris onto an accretion disk (Phinney 1989; Evans & Kochanek 1989).

Classical loss cone theory (Lightman & Shapiro 1977; Cohn & Kulsrud 1978), from which expressions like Eq. (6) were derived, was directed toward understanding the observable consequences of massive black holes at the centers of globular clusters, which are many relaxation times old. As Fig. 5 shows, few galactic nuclei are expected to be much older than T_r, and loss cone dynamics in galactic nuclei can therefore be very different than in globular clusters. For instance, in a nucleus that until recently contained a binary SBH, orbits of stars with pericenters $r_{peri} \lesssim a_h$ will have beeen depleted. The time required for gravitational encounters to repopulate these orbits is $\sim (a_h/r_h)T_r \approx (m_2/m_1)T_r$. For $m_2/m_1 = 0.1$, this time exceeds 10^{10} yr in most galaxies with $M_\bullet \gtrsim 10^8 M_\odot$ (Merritt & Wang 2005). Until the phase-space gap is refilled, tidal disruption rates can be much lower than in a collisionally-relaxed nucleus.

On the other hand, as Fig. 4 implies, loss-cone repopulation in a non-axisymmetric (triaxial or barred) nucleus can be much *more* efficient than repopulation due to gravitational encounters in the spherical geometry, due to the presence of centrophilic (box or chaotic) orbits in the triaxial geometry. Numerical integrations of centrophilic orbits show that the rate at which a single star experiences near-center passages with pericenter distances $\leq d$ is proportional to d (Gerhard & Binney 1985). In a $\rho \sim r^{-2}$ nucleus, the implied rate of supply of stars to the event horizon of the SBH is $\sim f_c\sigma^5/Gc^2$ where f_c is the fraction of orbits that are centrophilic. Even for modest values of f_c (~ 0.1), this collisionless mechanism can supply stars to the SBH at higher rates than collisional loss-cone repopulation, particularly in galaxies with $M_\bullet \gtrsim 10^7 M_\odot$ in which two-body relaxation times are very long (Merritt & Poon 2004). In fact, loss rates in the triaxial geometry can approach the so-called "full loss cone" feeding rates in spherical galaxies, which were invoked, in an early model, to explain QSO activity (Hills 1975; Young et al. 1977) and which have recently been revived (Zhao et al. 2002; Miralda-Escudé & Kollmeier 2005).

These arguments suggest that the mean rate of stellar tidal disruptions in galactic nuclei is poorly constrained by pure theory. One way to observationally constrain the disruption rate is via the X-ray luminosity function of active galaxies (Ueda et al. 2003; Barger et al. 2005; Hasinger et al. 2005). Assuming the $L_X \propto t^{-5/2}$ time dependence discussed above for individual events, and convolving Eq. (6) with the SBH mass function, one concludes (Milosavljevic, Merritt & Ho 2006) that tidal disruptions can account for the majority of X-ray selected AGN with soft X-ray luminosities below $\sim 10^{43} - 10^{44}$ erg s^{-1}.

Nearer to home, it might be possible to search for "afterglows" of the most recent tidal disruption event at the Galactic center, which could plausibly have occurred as little as $\sim 10^3$ yr ago (Eq. 6). Possible examples of such signatures include X-ray flourescence of giant molecular clouds (Sunyaev & Churazov 1998) and changes in the surface properties of irradiated stars (Jimenez et al. 2006).

Acknowledgements. I thank A. Graham for permission to reprint Fig. 3. This work was supported by grants from the NSF, NASA, and the Space Telescope Science Institute. Some of the computations described here were carried out at the Center for Advancing the Study of Cyberinfrastructure at the Rochester Institute of Technology.

References

Amaro-Seoane, P., Freitag, M., & Spurzem, R. 2004, MNRAS, 352, 655
Bahcall, J. N., & Wolf, R. A. 1976, ApJ, 209, 214
Ballo, L., Braito, V., Della Ceca, R., Maraschi, L., Tavecchio, F., & Dadina, M. 2004, ApJ, 600, 634
Barger, A. J., Cowie, L. L., Mushotzky, R. F., Yang, Y., Wang, W.-H., Steffen, A. T., & Capak, P. 2005, AJ, 129, 578
Baumgardt, H., Makino, J., & Ebisuzaki, T. 2004, ApJ, 613, 1133
Begelman, M. Blandford, R. D. & Rees, M. J. 1980, Nature, 287, 307
Berczik, P., Merritt, D., & Spurzem, R., ApJ, 633, 680
Berczik, P., Merritt, D., Spurzem, R., & Bischof, H.-P. 2006, ArXiv Astrophysics e-prints, arXiv:astro-ph/0601698
Boylan-Kolchin, M., Ma, C.-P., & Quataert, E. 2004, ApJ, 613, L37
Brown, W. R., Geller, M. J., Kenyon, S. J., & Kurtz, M. J. 2005, ApJ, 622, L33
Brown, W. R., Geller, M. J., Kenyon, S. J., & Kurtz, M. J. 2006, ArXiv Astrophysics e-prints, arXiv:astro-ph/0601580
Cohn, H., & Kulsrud, R. M. 1978, ApJ, 226, 1087
Donley, J. L., Brandt, W. N., Eracleous, M., & Boller, T. 2002, AJ, 124, 1308
Duncan, M. J., & Shapiro, S. L. 1983, ApJ, 268, 565
Escala, A., Larson, R. B., Coppi, P. S., & Mardones, D. 2004, ApJ, 607, 765
Escala, A., Larson, R. B., Coppi, P. S., & Mardones, D. 2005, ApJ, 630, 152
Evans, C. R., & Kochanek, C. S. 1989, ApJ, 346, L13
Favata, M., Hughes, S. A., & Holz, D. E. 2004, ApJ, 607, L5
Ferrarese, L., et al. 2006, ArXiv Astrophysics e-prints, arXiv:astro-ph/0602297
Ferrarese, L., & Ford, H. 2005, Space Science Reviews, 116, 523
Ferrarese, L. & Merritt, D., ApJ, **539**, L9
Frank, J., & Rees, M. J. 1976, MNRAS, 176, 633
Freitag, M., & Benz, W. 2002, A&A, 394, 345
Gebhardt, K., et al. 1996, AJ, 112, 105
Gebhardt, K., et al. 2003, ApJ, 583, 92
Genzel, R., et al. 2003, ApJ, 594, 812
Gerhard, O. E., & Binney, J. 1985, MNRAS, 216, 467
Graham, A. W. 2004, ApJ, 613, L33
Graham, A. W., Erwin, P., Caon, N., & Trujillo, I. 2001, ApJ, 563, L11
Gualandris, A., Zwart, S. P., & Sipior, M. S. 2005, MNRAS, 363, 223
Haehnelt, M. G., & Kauffmann, G. 2002, MNRAS, 336, L61
Halpern, J. P., Gezari, S., & Komossa, S. 2004, ApJ, 604, 572

Hasinger, G., Miyaji, T., & Schmidt, M. 2005, A&A, 441, 417
Hills, J. G. 1975, Nature, 254, 295
Hills, J. G. 1988, Nature, 331, 687
Hirsch, H. A., Heber, U., O'Toole, S. J., & Bresolin, F. 2005, A&A, 444, L61
Holley-Bockelmann, K., Sigurdsson, S., Mihos, J. C., Feldmeier, J. J., Ciardullo, R., & McBride, C. 2005, arXiv:astro-ph/0512344
Holley-Bockelmann, K., & Sigurdsson, S. 2006, ArXiv Astrophysics e-prints, arXiv:astro-ph/0601520
Jimenez, R., da Silva, J. P., Oh, S. P., Jorgensen, U. G., & Merritt, D. 2006, arXiv:astro-ph/0601527
Komossa, S. 2003, AIP Conf. Proc. 686: The Astrophysics of Gravitational Wave Sources, 686, 161
Komossa, S., Burwitz, V., Hasinger, G., Predehl, P., Kaastra, J. S., & Ikebe, Y. 2003, ApJ, 582, L15
Komossa, S., & Greiner, J. 1999, A&A, 349, L45
Komossa, S., Halpern, J., Schartel, N., Hasinger, G., Santos-Lleo, M., & Predehl, P. 2004, ApJ, 603, L17
Lightman, A. P., & Shapiro, S. L. 1977, ApJ, 211, 244
Makino, J., Fukushige, T., Koga, M., & Namura, K. 2003, PASJ, 55, 1163
Makino, J., & Funato, Y. 2004, ApJ, 602, 93
Marchant, A. B., & Shapiro, S. L. 1980, ApJ, 239, 685
Marconi, A. & Hunt, L.K. 2003, AJ, 589, L21
Merritt, D. 2006, Reports on Progress in Physics, in press
Merritt, D., Mikkola, S. & Szell, A. 2006, in preparation
Merritt, D., Milosavljević, M., Favata, M., Hughes, S. A., & Holz, D. E. 2004, ApJ, 607, L9
Merritt, D., & Poon, M. Y. 2004, ApJ, 606, 788
Merritt, D., & Szell, A. 2005, ArXiv Astrophysics e-prints, arXiv:astro-ph/0510498
Merritt, D., & Wang, J. 2005, ApJ, 621, L101
Meszaros, P., & Silk, J. 1977, A&A, 55, 289
Mikkola, S., & Valtonen, M. J. 1990, ApJ, 348, 412
Mikkola, S., & Valtonen, M. J. 1992, MNRAS, 259, 115
Milosavljević, M., & Merritt, D. 2001, ApJ, 563, 34
Milosavljević, M., & Merritt, D. 2003, ApJ, 596, 860
Milosavljevic, M., Merritt, D., & Ho, L.. 2006, arXiv:astro-ph/0602289
Milosavljević, M., Merritt, D., Rest, A., & van den Bosch, F. C. 2002, MNRAS, 331, L51
Miralda-Escudé, J., & Kollmeier, J. A. 2005, ApJ, 619, 30
Mortlock, D. J., Webster, R. L., & Francis, P. J. 1999, MNRAS, 309, 836
Phinney, E. S. 1989, IAU Symp. 136: The Center of the Galaxy, 136, 543
Poon, M. Y., & Merritt, D. 2004, ApJ, 606, 774
Preto, M., Merritt, D., & Spurzem, R. 2004, ApJ, 613, L109
Quinlan, G. D. 1996, New Astronomy, 1, 35
Rees, M. J. 1990, Science, 247, 817
Salpeter, E. E. 1964, ApJ, 140, 796
Sunyaev, R., & Churazov, E. 1998, MNRAS, 297, 1279
Ueda, Y., Akiyama, M., Ohta, K., & Miyaji, T. 2003, ApJ, 598, 886
Uttley, P. 2005, ArXiv Astrophysics e-prints, arXiv:astro-ph/0508060
Valluri, M., Merritt, D., & Emsellem, E. 2004, ApJ, 602, 66
Valluri, M., Ferrarese, L., Merritt, D., & Joseph, C. L. 2005, ApJ, 628, 137
Volonteri, M., Haardt, F., & Madau, P., ApJ, 582, 559
Wang, J., & Merritt, D. 2004, ApJ, 600, 149
Young, P. J., Shields, G. A., & Wheeler, J. C. 1977, ApJ, 212, 367
Yu, Q. 2002, *Mon. Not. R. Astron. Soc.*, **331**, 935
Zel'dovich, Y. B. & Novikov, I. D. 1964, Sov. Phs. Kokl., 158, 811
Zhao, H., Haehnelt, M. G., & Rees, M. J. 2002, New Astronomy, 7, 385